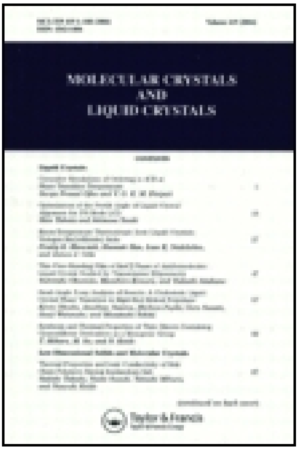

Molecular Crystals and Liquid Crystals Science and Technology. Section A. Molecular Crystals and Liquid Crystals

Publication details, including instructions for authors and subscription information:
http://www.tandfonline.com/loi/gmcl19

Crystal Structure and Properties of Dye-Containing Organic-Inorganic Perovskites

David B. Mitzi [a] & Konstantinos Chondroudis [a]

[a] IBM T.J. Watson Research Center, P.O. Box 218, Yorktown Heights, NY, 10598, USA

Version of record first published: 24 Sep 2006

To cite this article: David B. Mitzi & Konstantinos Chondroudis (2001): Crystal Structure and Properties of Dye-Containing Organic-Inorganic Perovskites, Molecular Crystals and Liquid Crystals Science and Technology. Section A. Molecular Crystals and Liquid Crystals, 356:1, 549-558

To link to this article: http://dx.doi.org/10.1080/10587250108023733

Mol. Cryst. and Liq. Cryst., 2001, Vol. 356, pp. 549-558
Reprints available directly from the publisher
Photocopying permitted by license only

Published by license under the
Gordon and Breach Science Publishers imprint.
Printed in Malaysia

Crystal Structure and Properties of Dye-Containing Organic- Inorganic Perovskites

DAVID B. MITZI and KONSTANTINOS CHONDROUDIS

IBM T.J. Watson Research Center, P.O. Box 218, Yorktown Heights, NY 10598 USA

The oligothiophene derivative, 5,5'''-bis(aminoethyl) 2,2':5',2'':5'', 2'''-quaterthiophene (AEQT), has been incorporated within a lead(II) halide-based perovskite framework. Single crystal X-ray analysis has been used to verify the perovskite framework and examine the ordering of the dye cations within the structure. Thin films of $(AEQT)PbX_4$ (X = Cl, Br, and I) have also been thermally ablated onto quartz substrates and the optical properties of the films have been examined. Strong photoluminescence from the quaterthiophene moiety is observed for X = Cl, with an emission peak at approximately $\lambda_{max} = 532$ nm. Similar photoluminescence is observed for the X = Br and I materials, but with progressively less intensity, as the band gap of the inorganic framework gets smaller relative to the LUMO-HOMO gap of the dye molecule. $(AEQT)PbCl_4$ films have also been incorporated as emission layers in light emitting devices (LED) and intense room temperature electroluminescence has been observed.

Keywords: organic-inorganic hybrid; perovskite; oligothiophene; electroluminescence; light-emitting device

INTRODUCTION

Crystalline organic-inorganic hybrid materials offer the possibility of combining useful properties of both organic (e.g. efficient and tunable luminescence, lightweight, easily processed) and inorganic (e.g. higher electrical mobility, thermal and mechanical stability) components within a single self-assembling molecular composite. Organic-inorganic perovskites [1] are one such structural family and exhibit a number of interesting physical properties, including tunable optical and electrical properties, as well as the possibility of being processed by simple techniques, such as spin-coating or single source thermal ablation [1, 2]. The $(C_4H_9NH_3)_2(CH_3NH_3)_{n-1}Sn_nI_{3n+1}$ (n = 1, 2, 3, ...) series, for example, consists of "n"-layer-thick tin(II) iodide based perovskite sheets separated by bilayers of butylammonium cations and undergoes a semiconductor-metal transition as a function of increasing perovskite sheet thickness [3]. The tin(II) and lead(II) halide based perovskites exhibit sharp, tunable peaks in the room temperature optical absorption and emission spectra [4]. These features arise from strongly bound (E_b > 200 meV) exciton states associated with the band gap of the metal halide framework and suggest possible application of the hybrid perovskites in light-emitting devices (LEDs). Recently, an LED employing $(C_6H_5C_2H_4NH_3)_2PbI_4$ as an emitter material has been demonstrated [5], producing highly intense green electroluminescence of more than 10,000 cd m^{-2} at liquid nitrogen temperature. Higher temperature operation results in quenching of the electroluminescence.

In most known hybrid perovskites, the organic layer of the structure plays a secondary role in distinguishing the interesting physical properties associated with each compound. For example, in the semiconducting/metallic halide-based perovskites [3], the organic layers serve to define the dimensionality of the compound. The highly conducting character, however, arises because of the small band gap in the metal halide sheets. These systems can in fact be considered self-assembling analogs to multilayer quantum well structures, consisting of semiconducting inorganic sheets alternating with much wider bandgap (insulating) organic layers. With regard to the strongly luminescent systems, the organic layers again serve to reduce the dimensionality of the structure and to further enhance the exciton binding energy through a "dielectric confinement" effect [6]. However, the photoluminescence arises from the radiative decay of excitons associated with the metal halide sheets. The large HOMO-LUMO energy gap for the relatively simple organic cation (alkylammonium or small aromatic ammonium) renders the molecules optically and electrically inert.

One motivation of the current study is to design an organic dye molecule that fits within the lead(II) halide based perovskite structure and that also plays a more active role in the electrical and optical properties of the hybrid. The issue of the resonant interaction between Wannier excitons in inorganic materials and Frenkel excitons in adjacent organic dye layers has recently been addressed theoretically and efficient energy transfer has been predicted in certain cases [7]. Incorporating the dye within an inorganic framework may also provide better thermal stability and charge transport properties for use in LEDs, compared to strictly organic dye materials. Better room temperature electroluminescence efficiency can also be expected compared to the non-dye-containing organic-inorganic perovskites.

RESULTS AND DISCUSSION

A number of structural factors influence the design of more complex (i.e. compared to alkylammonium or simple aromatic ammonium) organic cations for incorporation within the layered perovskite framework [1]. First, the molecule must contain one or two unobstructed ammonium units (or other cationic hydrogen bonding components) so that reasonably strong hydrogen bonding can occur between these groups and the perovskite sheet halogens. One straightforward way to insure this interaction is to attach the ammonium group using a sufficiently long alkylammonium chain – that is either as $R\text{-}(CH_2)_nNH_3^+$ or as $^+H_3N(CH_2)_n\text{–}R\text{–}(CH_2)_nNH_3^+$ with $n \geq 2$. For the monoammonium cations, the organic cations hydrogen bond to only one inorganic layer, providing for a bilayer of organic cations between the perovskite sheets and a van der Waals gap between the layers. For the diammonium cations, the organic cations span the entire distance between and bond to two adjacent inorganic sheets.

A second factor influencing the suitability of a given organic cation for the perovskite structure is the shape of the molecule. The projection of the organic cation on a plane along one axis of the molecule (or the "cross-sectional area" of the cation) must fit within the nominally square area defined by the terminal halogens from four adjacent corner-sharing octahedra. One edge of the square is approximately twice the average bridging interatomic M – X distance. For the lead(II) bromide framework, this square provides an area of ~35 Å^2. If the "cross-sectional area" of the organic molecule is much smaller than this square, the structure can accommodate the discrepancy by allowing the organic molecules to tilt or interdigitate. On the other hand, if the area required by the organic molecule is too large, the perovskite structure is not able to adapt and a different structural type will result. For the layered perovskite framework, organic molecules with a long and narrow profile are therefore preferable to those that are wide and bulky.

Finally, in the solid state, interactions between the "R" groups of the organic cations, R - $(CH_2)_nNH_3^+$ or $^+H_3N(CH_2)_n$ – R – $(CH_2)_nNH_3^+$, can influence the overall structure and ultimately either stabilize or destabilize the perovskite framework. The polymerized (HOOC-CH=CH-CH=CH-$CH_2NH_3)_2CdCl_4$ perovskite structure, for example, is stabilized by hydrogen bonding between COOH groups on adjacent organic sheets [8]. Other types of interactions that can influence the overall organic-inorganic structure include van der Waals and aromatic-aromatic interactions between the "R" groups.

The oligothiophenes are particularly interesting molecules for potential incorporation in perovskites because of the long and relatively rigid nature of the molecule and because the energy at which the molecules absorb (and subsequently emit) light can be controlled by choosing the length of the thiophene chain. The lead(II) halide based layered perovskites (with optically inert organic cations) exhibit a strong peak in the absorption spectrum at 332 nm (3.7 eV) for X = Cl, 405 nm (3.1 eV) for X = Br, and 504 nm (2.5 eV) for X = I, as a result of exciton states associated with the inorganic sheet band gap [1]. The absorption maximum for "n" α-linked thiophene rings varies between approximately 302 nm (4.1 eV) for n = 2 to 432 nm (2.9 eV) for n = 6 [9]. For quaterthiophene, the peak absorption comes at approximately 390 nm (3.2 eV). This molecule is therefore an interesting choice for incorporation within the lead(II) halide based organic-inorganic perovskite structures. For X = Cl, the inorganic layer exciton peak falls at a higher energy than the quaterthiophene absorption peak. For X = Br, the energy levels are approximately equal, while for X = I, the energy of the exciton state in the inorganic framework is lower than that for the quaterthiophene moiety. This series of compounds is therefore expected to enable an examination of energy transfer between the dye and the inorganic framework. Considering both the structural and energy level requirements for the oligothiophene derivative, 5,5'''-bis(aminoethyl)-2,2':5',2'':5'',2'''-quaterthiophene (AEQT), was selected for incorporation within the hybrid perovskite framework.

The synthesis of the AEQT molecule and crystal growth of the $(AEQT)PbX_4$ crystals will be described elsewhere [1, 10]. The crystal structure of $(AEQT)PbBr_4$ at room temperature is shown in Figure 1 and consists of anionic sheets of corner-sharing $PbBr_6$ octahedra separated by a layer of $AEQT^{2+}$ cations. The new compound adopts a monoclinic (*C2/c*) cell with the dimensions a = 39.741(2) Å, b = 5.8420(3) Å, c = 11.5734(6) Å, and β = 92.360(1)°. Evidence of a partially ordered superstructure is observed from the X-ray data [10].

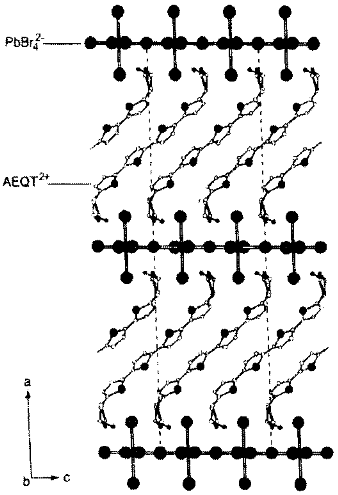

FIGURE 1. Crystal structure of (AEQT)PbBr$_4$ viewed down the *b*-axis. The unit cell outline is shown by the dashed lines.

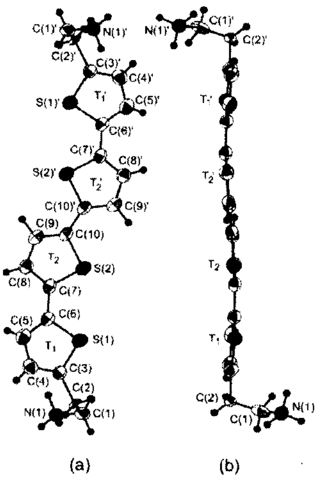

FIGURE 2. Top (a) and side (b) view of the doubly protonated AEQT cation in the (AEQT)PbBr$_4$ structure.

The conformation of the protonated 5,5'''-bis(aminoethyl)-2,2':5',2'':5'',2'''-quaterthiophene molecule in (AEQT)PbBr$_4$ is shown in Figure 2. Each quaterthiophene oligomer can be fully described by two independent thiophenes rings, T$_1${S(1), C(3), C(4), C(5), C(6)} and T$_2${S(2), C(7), C(8), C(9), C(10)}. The other half of the quaterthiophene oligomer is generated by symmetry from the *C2/c* space group, yielding the rings T$_1$'and T$_2$'. The backbone conformation among the four rings is *syn-anti-syn*. Each thiophene ring is essentially planar, with all non-hydrogen atoms falling within 0.01(1) Å of the least squares best-plane. The dihedral angle between the planes defined by the two thiophene rings, T$_1$ and T$_2$ (or T$_1$' and T$_2$'), is 9.0(2)°. This angle is accomplished by a combination of a tilting of the connecting C(6)-C(7) [C(6)'-C(7)'] bond, out of the plane of the central two thiophene rings (T$_2$ and T$_2$'), as well as by a rotation about this bond axis.

The *syn-anti-syn* geometry is somewhat uncommon among the oligothiophenes. Generally, as a result of steric interactions, the all-*anti* (or all-*trans*) geometry can be regarded as the lowest energy configuration [11]. In the solid state, the all-*anti* conformation is adopted for α-quaterthiophene [12], 5,5'''-bis[(2,2,5,5-tetramethyl-1-aza-2,5-disila-1 - cyclopentyl)methyl] - 2,2':5',2'':5'',2''' - quaterthiophene, and 5,5'''-bis[N,N-bis(tri-methylsilyl)aminomethyl]-2,2':5',2'':5'',2'''-quaterthiophene [13]. However, 5,5'''-bis[(2,2,5,5-tetramethyl-1-aza-2,5-disila-1-cyclopentyl)ethyl] - 2,2':5',2'':5'',2''' - quaterthiophene has recently been shown [13] to adopt a nearly planar (dihedral angle of 5.0° between least-squares best planes containing adjacent thiophene rings) *syn-anti-syn* conformer, similar to that observed in $(AEQT)PbBr_4$.

The quaterthiophene oligomers pack into the layered organic-inorganic framework such that the quaterthiophene units are tilted relative to the perovskite sheet normal. The least squares plane through the quaterthiophene section of the AEQT molecule (averaging over the slight misorientation of the planes defined by the T_1 and T_2 rings) provides a dihedral angle of 44.53(6)° with respect to the plane containing the perovskite sheets. Viewing down the length of the quaterthiophene molecules, the oligomers in $(AEQT)PbBr_4$ adopt an herringbone arrangement (Figure 3), similar to that observed in purely organic crystals and films of the various oligothiophenes [14-16]. The closest contacts between quaterthiophene oligomers include $C(7)\cdots C(9)^*$ [3.580(9) Å] and $S(2)\cdots C(8)^*$ [3.586(8) Å]. These values are close to the sum of the van der Waals radii for each atom (~ 1.7 Å for carbon and ~ 1.8 Å for sulfur [17]). The closest intermolecular S···S interaction is $S(1)\cdots S(2)^*$ [4.148(3) Å]. More complete structural details for $(AEQT)PbBr_4$, including atomic coordinates and bond angles and distances, will be published separately [10].

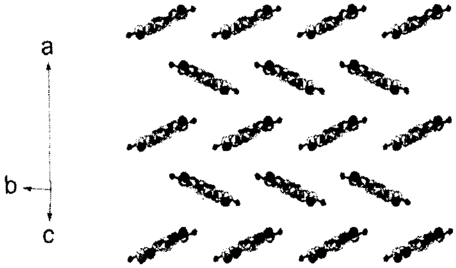

FIGURE 3. View down the long molecular axis of one layer of AEQT cations in $(AEQT)PbBr_4$. For clarity, only the quaterthiophene component of each cation is drawn.

Figure 4 shows the optical absorption spectra for (AEQT)PbX_4 (X = Cl, Br, I) thin films (1000-1500 Å thick) prepared by single source thermal ablation and low-temperature annealing (<200°C for 15 min) [2]. The exciton peak associated with the bandgap of the lead(II) halide sheets is clearly evident in each spectrum, demonstrating that the perovskite structure has been formed for each of the films. For X = Cl, Br, and I, the exciton peak falls at approximately 331, 404, and 524 nm, respectively. These values are characteristic of the inorganic perovskite layers for each halide and are similar to the values observed for the non-dye-containing organic-inorganic perovskites [1]. In addition to the exciton peak, a broader absorption peak at approximately 385 nm can be observed in each spectrum from the quaterthiophene cation [9]. The photoluminescence spectrum for the X = Cl perovskite film is shown in Figure 5 and exhibits a strong peak from the quaterthiophene moiety at 532 nm. Photoluminescence from quaterthiophene in the X = Br and I compounds drops precipitously in intensity across the series from X = Cl to X = I. Although the details of the quenching mechanism are still not fully understood, the mechanism presumably involves the reduction of the inorganic layer bandgap to a value lower than the HOMO-LUMO gap in the quaterthiophene layer, and the subsequent energy transfer between the organic and inorganic components.

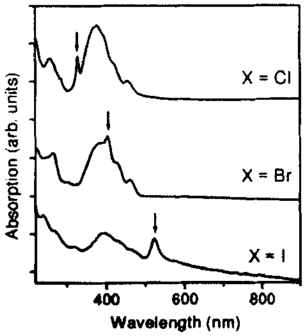

FIGURE 4. Room temperature UV-Vis absorption spectra for thermally ablated and annealed films of (AEQT)PbX_4 (X = Cl, Br, I).

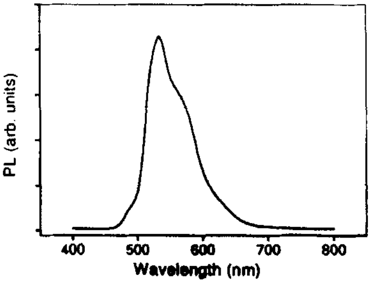

FIGURE 5. Room temperature photoluminescence(PL) emission spectrum (λ_{ex}= 360 nm) for a thermally ablated and annealed film of (AEQT)PbCl_4.

An LED containing the organic-inorganic perovskite (AEQT)$PbCl_4$ has also been constructed [18]. The device (Figure 6, inset) consists of a circular (¾" diameter) quartz substrate on which indium tin oxide (ITO) has been e-beam deposited (1500 Å, 14 Ω/square). To avoid shorting between the anode and cathode, 1300 Å of SiO_2 was deposited on top of the ITO through contact masks that define four rectangular areas (3 x 1 mm) of exposed ITO. The patterned substrates were cleaned by ultrasonication for 5 min in each of the following: 1 % w/v aqueous detergent solution, acetone and methanol, and then boiled in methanol for 5 min. They were dried in a 120°C oven and subjected to an O_2 plasma (30 W, 120 mTorr, 4 min). A 3000 Å (AEQT)$PbCl_4$ film was then deposited by single source thermal ablation under a vacuum of 10^{-7} Torr and annealed at low temperature [2]. Subsequently, 200 Å of the electron-transporting 1,3,4-oxadiazole,2,2'-(1,3-phenylene)bis[5-[4-(1,1-dimethylethyl)phenyl]] (OXD7) was deposited by resistive heating at 10^{-7} Torr. To complete the devices, an alloy of $Mg_{20}Ag$ was deposited by coevaporation (600 Å), followed by another 1200 Å of Ag to inhibit oxidation. The $Mg_{20}Ag$/Ag cathode was deposited through contact masks with rectangular 2 x 7 mm openings. The openings are at 90° to the exposed ITO areas, therefore defining an active device area of 1 x 2 mm. The devices were processed in a nitrogen atmosphere and encapsulated using a cover glass and epoxy before testing.

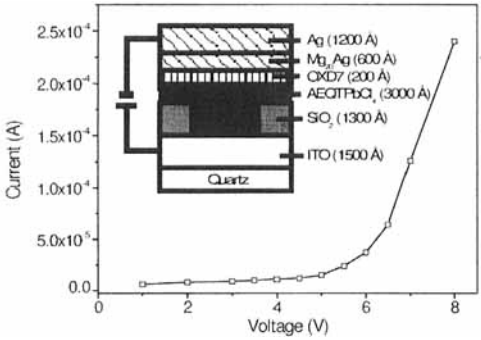

FIGURE 6. I-V curve for an OILED structure based on (AEQT)$PbCl_4$. The inset shows a cross sectional view of the device used in the study.

Figure 6 shows the current voltage (I-V) characteristics of the organic-inorganic LED (OILED) structure. Bright green luminescence (λ_{max}=530 nm) was observed in a well-lit room when the devices were forward biased under ambient conditions. A low turn-on voltage of approximately 5.5 V was observed, despite the relatively thick (AEQT)$PbCl_4$ emission layer. The electroluminescence spectrum corresponds well to the photoluminescence spectrum of (AEQT)$PbCl_4$ (Figure 7). The maximum efficiency was 0.1 lm/W at 8 V and 0.24 mA. In contrast to devices with non-dye-containing hybrid perovskites, the current devices operate with reasonable efficiency at room temperature. The observed efficiency also compares favorably to the values achieved for devices made with purely organic oligothiophene derivative emission layers (≤ 0.03 lm/W [19]).

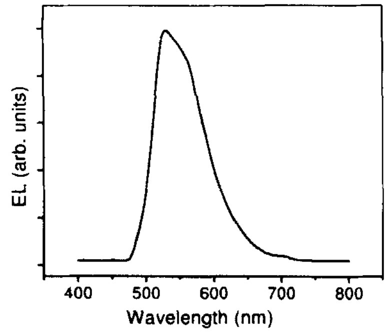

FIGURE 7. Room temperature electroluminescence spectrum for the OILED shown in Figure 6 (inset). The device is driven at 8 V.

CONCLUSION

An organic-inorganic perovskite containing an oligothiophene dye derivative has been achieved. The inorganic perovskite framework templates the ordering of the dye cations, resulting in single layers of ordered quaterthiophene oligomers positioned between inorganic sheets of lead(II) halide. Strong photoluminescence has been observed from the dye molecules in the lead(II) chloride framework. In addition, an LED has been demonstrated employing (AEQT)$PbCl_4$ as the emission layer. The unoptimized devices exhibit an efficiency that is larger than typically observed for devices made with neutral oligothiophene dye molecules (with no inorganic framework). Significantly, the oligothiophene-containing perovskite layers can be made quite thick (~ 3000 Å), compared to most organic LED materials. This suggests reasonable charge transport properties for the hybrids. Whereas in the current example green electroluminescence has been demonstrated, the hybrid structures can be generalized to contain dye molecules that luminesce in other regions of the spectrum. Other inorganic frameworks (with different band gap) can also be substituted for lead(II) halide.

ACKNOWLEDGMENTS
The authors wish to thank DARPA for partial support of this work under contract DAAL01-96-C-0095.

References

[1] For a review, see: D.B. Mitzi, *Prog. Inorg. Chem.* **48,** 1 (1999).
[2] D.B. Mitzi, M.T. Prikas, K. Chondroudis, *Chem. Mater.* **11,** 542 (1999); K. Chondroudis, D.B. Mitzi, *Chem. Mater.*, in press.
[3] D.B.Mitzi, C.A. Feild, W.T.A. Harrison, A.M. Guloy, *Nature* **369,**467 (1994).
[4] T. Ishihara, in *Optical Properties of Low-Dimensional Materials,* T. Ogawa and Y. Kanemitsu, Eds., World Scientific, Singapore, 288–339 (1995); G. C. Papavassiliou, I. B. Koutselas, *Synth. Metals* **71,** 1713 (1995).
[5] M. Era, S. Morimoto, T. Tsutsui, S. Saito, *Appl. Phys. Lett.* **65,** 676 (1994).
[6] X. Hong, T. Ishihara, A.V. Nurmikko, *Phys. Rev. B* **45,** 6961 (1992).
[7] V.M. Agranovich; D.M. Basko, G.C. La Rocca, F. Bassani, *J. Phys.: Condens. Matter* **10,** 9369 (1998); V.M. Agranovich, G.C. La Rocca, F. Bassani, *JETP Lett.* **66,** 748 (1997).
[8] B. Tieke, G. Chapuis, *Mol. Cryst. Liq. Cryst.* **137,** 101 (1986).
[9] D. Grebner, M. Helbig, S. Rentsch, *J. Phys. Chem.* **99,** 16991 (1995).
[10] D. B. Mitzi, K. Chondroudis, C. R. Kagan, *Inorg. Chem.*, in press.
[11] V. Barone, F. Lelj, N. Russo, M. Toscano, *J. Chem. Soc. Perkin Trans. II,* 907 (1986).
[12] T. Siegrist, C. Kloc, R. A. Laudise, H. E. Katz, R. C. Haddon, *Adv. Mater.* **10,** 379 (1998).
[13] H. Muguruma, K. Kobiro, S. Hotta, *Chem. Mater.* **10,** 1459 (1998).
[14] L. Antolini, G. Horowitz, F. Kouki, F. Garnier, *Adv. Mater.* **10,** 382 (1998).
[15] T.M. Barclay, A. W. Cordes, C. D. MacKinnon, R. T. Oakley, R. W. Reed, *Chem. Mater.* **9,** 981 (1997).
[16] S. Hotta, K. Waragai, *Adv. Mater.* **5,** 896 (1993).
[17] A. Bondi, *J. Phys. Chem.* **68,**441 (1964).
[18] K. Chondroudis, D.B. Mitzi, *Chem. Mater.* **11,** 3028 (1999).
[19] K. Uchiyama, H. Akimichi, S. Hotta, H. Noge, H. Sakaki, *Synth. Met.* **63,** 57 (1994); T. Noda, H. Ogawa, N. Noma, Y. Shirota, *Adv. Mater.* **9,** 720 (1997).